

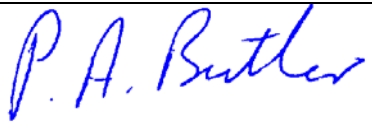
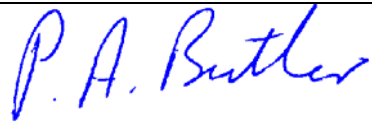
CONTRACT N°: RII3-CT-2004-506065

ISSUE CERTIFICATE

EURONS

EUROpean Nuclear Structure research

Activity *JRA06: INTAG*Identification: *D-J06-3.1*Revision: *0**Task report*Dissemination level: *R/PU*Issued by: *U Liverpool*Reference: *EURONS-D-J06-3.1*Status: *Final*Summary:*Report on task T-J06-3 (Application of tagging method to in-flight separated beams)*

	Peter Butler (U Liverpool)	Peter Butler (U Liverpool)	Alex C. Mueller, CNRS
8.12.2008			
DATE	RESPONSIBLE Name/Company Signature	WP LEADER Name/Company Signature	COORDINATOR Name/Company Signature

T-J06-3

Final Report

Application of tagging method to in-flight separated beams

- ▶ **Objectives**
- ▶ **T-J06-3.1 – Ge detectors**
 - ▶ *Design of the segmented planar*
 - ▶ *Scanning tables for Ge detectors*
- ▶ **T-J06-3.2 - Tracking detectors**
 - ▶ *Simulations for slow down beams at FRS*
 - ▶ *Coulomb excitation analysis for slow down beam at GSI*
 - ▶ *Manufacturing and testing of tracking detectors*
 - ▶ *Momentum selection of spin-aligned isomeric beams in the FRS spectrometer*
- ▶ **Conference presentations**

- ▶ **Milestone table**

T-J06-4 - Objectives

The task is centered on FRS-RISING facility at GSI Darmstadt. The magnetic spectrometer FRagment Separator coupled to the RISING γ array allows to study radioactive decay and Coulomb excitation of short-lived exotic nuclei, selected by RDT following fragmentation of relativistic beams, slowing or stopping of beams. Its goal is the design of the optimum configuration for a RTD setup to study multiple Coulomb excitation, resonance and transfer reactions following slow down fragmentation products. Here account has to be taken for the very large beam emittance (energy and angular spread), requiring tracking before and after the scattering event. Future employment of planar Ge tracking detectors will allow an improvement the quality of γ -ray spectra associated with radioactive ions. The design study of such detectors was the other goal of this task.

T-J06-3.1 - Ge detectors

DESPEC setup will incorporate high efficiency and highly segmented Ge detectors in close-packed geometry around the stopping volume for the ions. Most demanding is the observation of the gamma decay of implanted nuclei from isomeric nuclear states, because the implanted particle has to be associated with the subsequent gamma emission. For isomer decay times of more than typically 100 ms uncorrelated gamma-rays originating from background sources may become dominant, reducing the peak-to-background (P/B) ratio of the decay gamma-spectrum. A novel method to reduce the background uses the imaging capability of the planned detector array to trace the origin of the gamma rays back to the implantation target [1]. Rejecting gammas not originating from the target area is a powerful tool to optimize the P/B ratio. A new generation of highly segmented, high purity germanium detectors with 3D position sensitivity based on the well established technique of pulse shape analysis (PSA) provide excellent possibilities for gamma tracking. Based on these principles a prototype detector unit is being designed which consists of three planar double-sided Ge strip detectors arranged in a telescope with 6mm gap between the crystals.

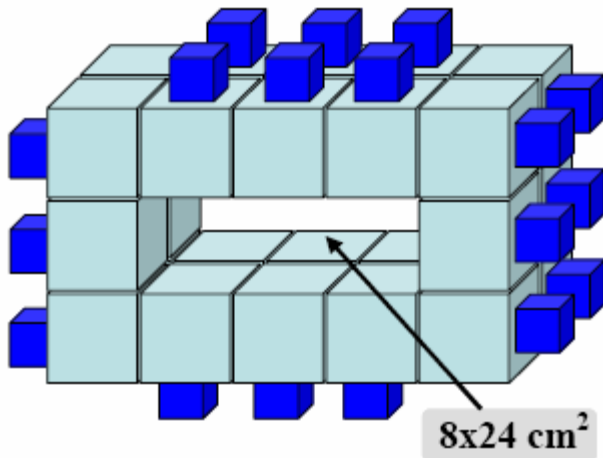


Figure 1 Possible geometries of the proposed Ge array consisting of 24 detector units.

We propose a highly flexible and modular high-resolution γ -ray detection array consisting of 24 stacks of planar double-sided Ge strip detectors as shown in Figure 1. These modules can be arranged in different geometries optimized to the different types of experiments envisaged at DESPEC. The high granularity of the Ge detectors is important in order to assure high efficiency of the array during the "prompt flash" of radiation associated with the implantation of high energy ions into the focal plane catcher and thus to allow the study of decays with very short lifetimes. In addition the granularity allows us to track the origin of the detected γ -ray. This tracking allows us to associate an implanted ion with its decay γ -rays (excluding random coincidences with background radiation produced upstream) and, hence, enables long decay times to be studied at high implantation rates. In addition the position information can be used to measure angular correlations and polarizations.

Design of the segmented planar Ge: GSI

The proposed design is based on a detector element produced at the FZ Jülich of a size of 72×72 mm² and a thickness of 20 mm. Due to a guard ring around the detector the active surface is 68×68 mm². A strip pitch of 8.5 mm leads to 8×8 pixels per detector element and requires 16 channels of read-out electronics. Applying simple pulse shape analysis it is expected to be possible to obtain a depth resolution of about 7 mm, resulting in 192 voxels per detector element. A stack of three such elements mounted in a common cryostat forms a detector unit. The array shown in Figure 1 consists of two rings of 12 units each on both sides of the active catcher in the focal plane which is assumed to have a size of 8×24 cm². The expected efficiency of the setup is superior to the existing gamma arrays and additionally the imaging capability allows for background reduction as it was demonstrated [1]. Monte-Carlo simulations of the prototype detector unit for the DESPEC Ge array showed its high background suppression capabilities. The number of events from background sources can be reduced by a factor of 10 while keeping 80% of the full-energy events from the “target” source. Compromising the full-energy efficiency this factor can rise up to 100 or more. Additionally the P/T for the “target” spectrum can be significantly increased.

The design of a cryostat for one planar detector is shown in Figure 2. In the future the very compact assembly has to accommodate two further crystals.

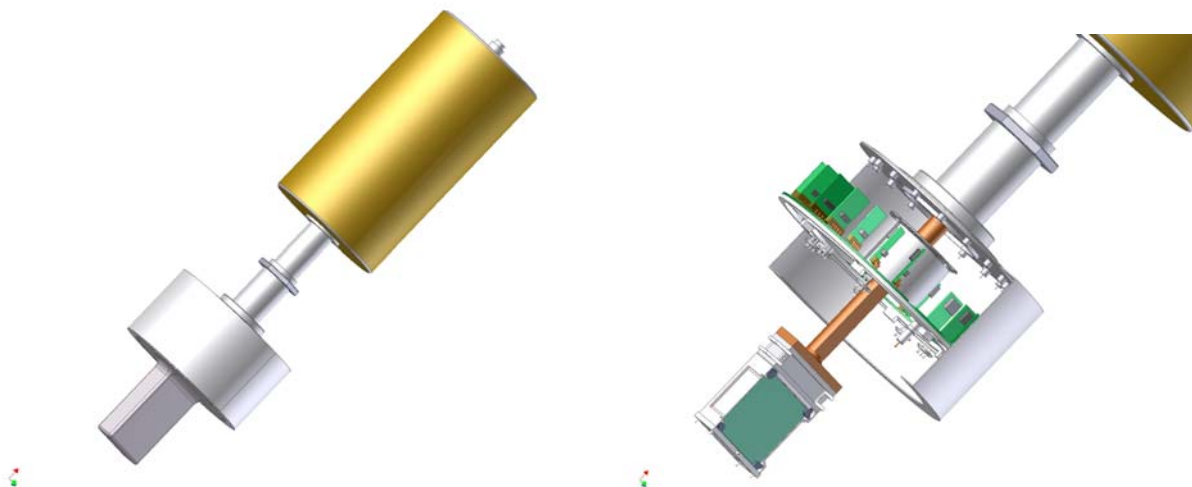


Figure 2 Design of planar Ge single cryostat. This design assumes a stack of three planar Ge detectors placed in a close geometry.

Scanning tables for Ge detectors: IPHC Strasbourg, GSI, IN2P3

Segmented Ge detectors may be used as position sensitive detectors. Indeed, the preamplifier pulse shapes vary relative to the spatial position of the gamma-ray interaction points in the Ge crystal. This enables the gamma-ray path reconstruction and the determination of the source emission point. This property will be used in the DESPEC array to trace back the implantation points on the focal plane emitting the detected gamma rays.

Such gamma-ray reconstruction is performed in two steps:

- The pulse shape analysis to determine the interaction point coordinates and the corresponding energy deposits
- The gamma-ray tracking.

The former is possible when the Ge detector response has been calibrated by a preliminary crystal 3D scanning using a scanning table. Such a table delivers a collimated gamma-ray beam in X and Y coordinates. The beam crosses the Ge crystal. Gamma rays scattered perpendicularly to the beam are detected in a scintillator detector which determines the Z coordinates. For each such scintillator-Ge coincidences, the pulse shapes of all Ge segments and of the full energy contact are recorded in

a database which will be used by the pulse shape analysis algorithm.

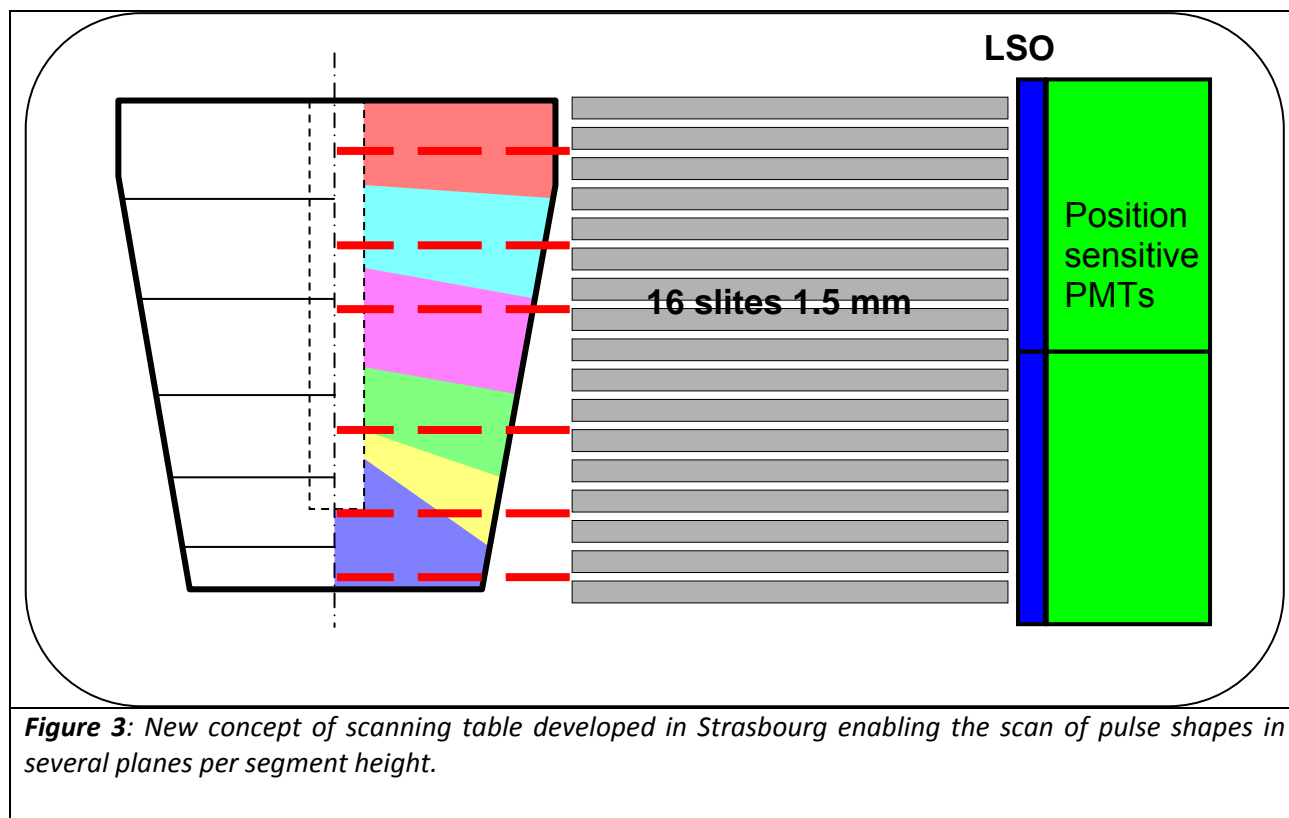


Figure 3: New concept of scanning table developed in Strasbourg enabling the scan of pulse shapes in several planes per segment height.

The unique scanning table presently operational in Europe is in Liverpool, UK. It enables the scan of AGATA detectors which are segmented in 6 sectors and 6 slices. Pulse shapes are measured in only one plane (one Z value) per slice or segment height. A new concept of scanning table has been developed in Strasbourg (see figure 3) which enables in a single measurement to record pulse shapes in 2 to 3 planes per segment height. This principle applies to any type of detector scanned in particular planar detectors of interest for DESPEC.

The new concept is based on the use of a large scintillator crystal (dark blue in figure 3) optically connected to position sensitive photomultipliers (green in figure 3) which photocathode is segmented in 8x8. The scintillator crystal covers the whole surface behind the lateral collimator slits. The light position produced by the detection of the gamma ray in the scintillator detector is obtained by weighting each photocathode segment position by the corresponding light collected. Preliminary tests have been performed with a thin (3 mm) GSO crystal and a 2inchx2inch active surface 8x8 segmented Hamamatsu PMT. The position sensitivity of the whole system has been determined by varying the slit-to-slit distance (see figure 2 A and B). The optimal separation between slits is 4mm (see figure 2 B and C). With such a scanning table design, measurements in 5 depth planes are possible for a 20 mm thick planar Ge crystal. Pulse shapes are recorded using TNT2 digital-electronics cards developed in Strasbourg [2, 3] which sample the preamplifier pulses with 100 MHz-14 bits flash ADCs. The incident gamma ray is the 662 keV transition from ^{137}Cs source, the scattered gamma ray has an energy of 288 keV (scattering at 90°) and the remaining energy in the Ge is 374 keV. Scintillator-Ge coincidences are requested to happen in a time window of 300ns. In the Ge detector, an energy window of ± 5 keV is imposed off line around 374 keV to preferentially select the events of interest and get rid of the background cosmic rays. The many pulses recorded are time aligned and averaged (see figure 4) before incrementing the pulse shape database. The spread of the rise times and the slightly different slopes are related to the gamma-ray spot size, about 3mm, at the interaction point.

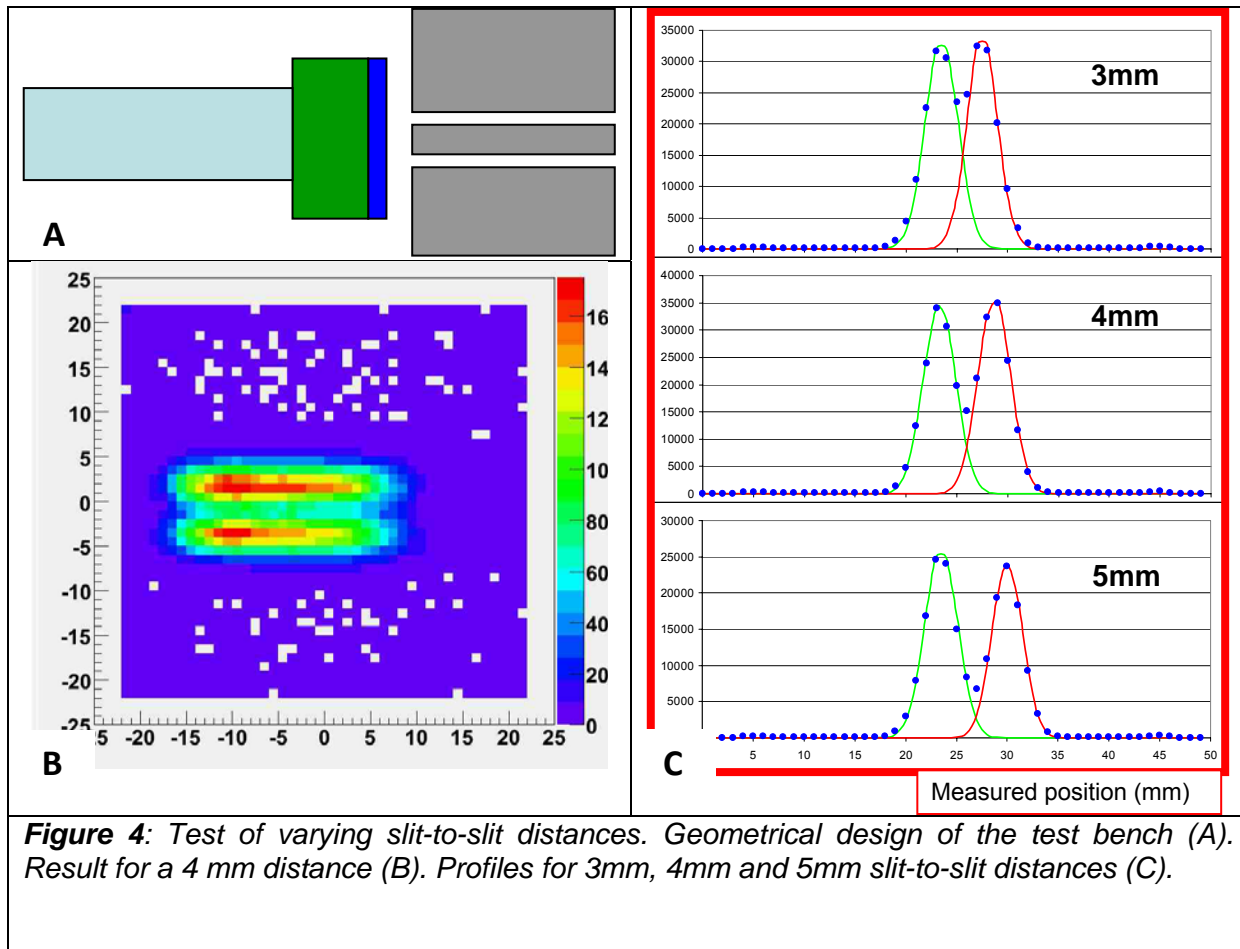


Figure 4: Test of varying slit-to-slit distances. Geometrical design of the test bench (A). Result for a 4 mm distance (B). Profiles for 3mm, 4mm and 5mm slit-to-slit distances (C).

T-J06-3.2 - Tracking detectors

Nuclear structure studies performed at **Coulomb barrier energies** have benefited largely from 4π Ge detector arrays such as EUROBALL, JUROGAM, GASP, EXOGAM and MINIBALL in Europe and GAMMASPHERE in the USA, in which a key component was an efficient, ancillary charged-particle array. The main experimental considerations are related to reaction channel selection to enable the search for weakly produced exotic nuclei or structures, and exclusive determination of the reaction kinematics for improved γ - and particle energy resolution. The application of this method to the in-flight separated beams requires identification of the beam particle and reaction products event by event.

Significant progress in prompt γ -ray spectroscopy of rare nuclei was achieved at the RISING setup in GSI due to availability of relativistic radioactive ion beams (RIBs) produced in flight [4]. In addition, delayed γ -decay studies of stopped fragments at RISING were successful [5]. However, use of RIBs slowed down to a Coulomb barrier energy would open a new perspective in in-beam - spectroscopy studies of nuclei far off stability accessible by resonance, transfer reactions, deep inelastic collisions and, in some cases, fusion-evaporation reactions. At the planned radioactive beam facility NUSTAR we aim at high resolution -spectroscopy measurements with secondary RIBs at energies close to the Coulomb barrier limit of 5 MeV/u. Relativistic radioactive fragments created in flight will be selected and slowed down in a series of degraders. In turn, they will induce a nuclear reaction on a target. The secondary beam intensity can reach 10^7 particles/s. However, a significant spread in the projectile energy and position is expected. Detection of prompt -radiation emitted from the reaction target will

employ novel techniques that incorporate pulse shape analysis and tracking of scattered photons. Nonetheless, for efficient Doppler shift compensation exact information about the velocity vector and the position of every projectile at the target has to be determined. Detectors suitable for the RIB tracking shall provide: (i) good energy resolution and minimum ion energy absorption, (ii) excellent timing properties, (iii) high efficiency and low dead-time, (iv) radiation hardness.

Simulations for slow down beams at FRS:(GSI)

The slowed down setup at FRS utilizes a thick degrader positioned after the fragment separator. The ions of interest are tracked and identified before the slowing down with the detectors available at FRS [6]. After the degrader the fragments enter an evacuated tube and are detected in a transmission position sensitive Time Of Flight (TOF) detector, positioned 1.5 m down stream. The measured TOF and position are used to determine the ions velocity and trajectory on even-by-event basis.

A Monte Carlo(MC) simulations showed that 80% on the fragments survive the slowing down process. The simulation predicted that the majority of the fragments created due to fragmentation reactions into the degrader have different velocity compare to the ions of interest. Figure 5 shows the calculated yield due to reactions into the degrader when ^{62}Co fragment is slowed down to 10 MeV/u. The MC simulation predicted that ^{62}Co will dominate by three orders of magnitude the ions created due to reactions in the degrader when a TOF gate corresponding to energy of 10 MeV/u is applied. Hence, only a TOF measurement was considered for the experiments with slowed down beams at FRS.

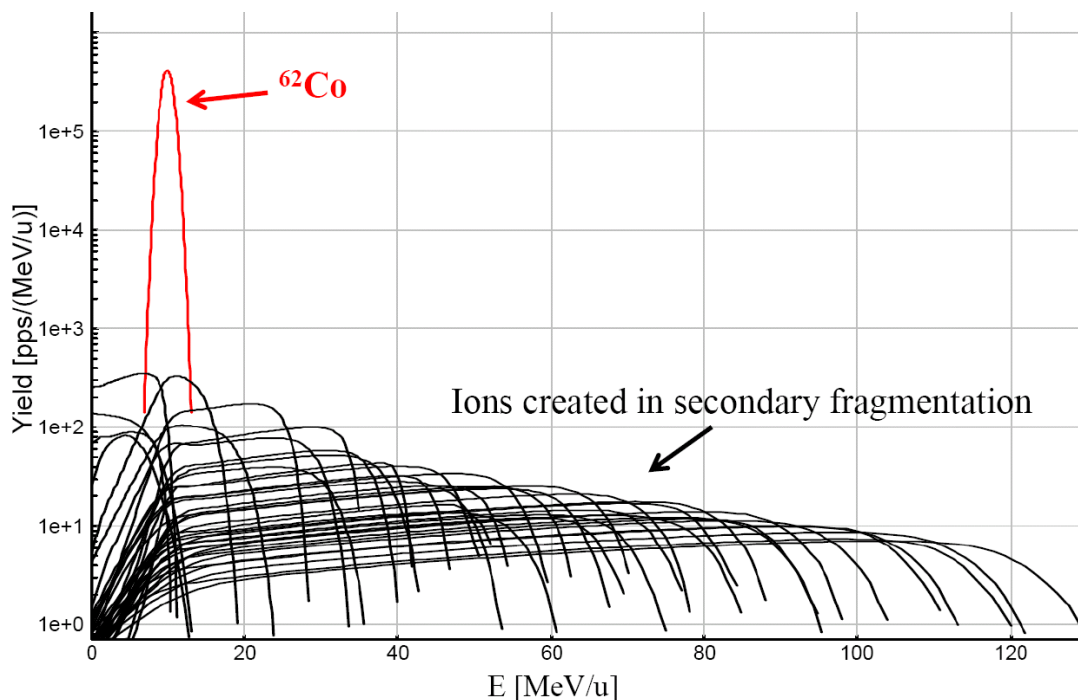


Figure 5: A simulation of the velocity distribution of the fragments created when ^{62}Co is slowed down to 10 MeV/u. The square root of the energy per nucleon is proportional to the fragment velocity. The contaminants from secondary reactions are of the order of 10^{-3} compared to the fragment of interest.

Several different types of position sensitive TOF detectors were considered for the slow down beam measurement. The expected gamma ray Doppler broadening $\delta E_\gamma / E_\gamma$ after TOF and position reconstruction was used to select the best candidate. In order to remove the uncertainty due to the energy loss into the TOF detector, it was assumed what the energy loss into the detector will be added to the reconstructed energy from TOF on event by event basis, when possible.

The considered detectors were position 1.5m behind the degrader. Under these conditions the Doppler broadening is as follows:

- Scintillator, 100 μm , no energy loss information:
 $\delta E_\gamma / E_\gamma = 0.02$
- Diamond, 40 μm , no energy loss information:
 $\delta E_\gamma / E_\gamma = 0.05$
- Si, 40 μm , 100ps time resolution and 1% energy resolution, energy loss added back
 $\delta E_\gamma / E_\gamma = 0.017$
- Secondary Electron Detectors, 150 ps time resolution (negligible energy loss)
 $\delta E_\gamma / E_\gamma = 0.0075$

A diamond detector of thickness of 40 μm is expected to introduce energy straggling of order of $\delta E=300$ MeV and angular straggling of $\delta\theta =2$ mrad. With the current diamond technology we can not obtain 5x5cm mono-crystal, hence we can not measure the energy loss in the detector to compensate for the energy straggling. The expected Doppler shift broadening is 0.05, which is worse than what we can obtain with a scintillator. Hence a much thinner crystal is needed.

From the detectors mentioned above, Secondary Electron, PPAC or fast Si detector are good candidates for the slow down beam measurement. The first two detectors are the thinnest of the detectors which were considered. A position sensitive PPAC may be limited to rates of order of $\sim 10^5$, while a MCP could operate at higher rates. A Si detector provides ΔE information which is sufficient to separate beam contaminants with different Z, but it has smaller radiation hardness compared to MCP or PPAC.

The beam spot size is another limiting factor to consider. Slower detectors require larger flight path after the degrader, and therefore larger active area. The calculated angular straggling due to slowing down is FWHM ~ 20 mrad. In the RISNG FRS setup the center of the RISING Ge array is at a distance of 1.5 m behind the degrader. This corresponds to a beam spot FWHM of 3 cm.

Coulomb excitation analysis for slow down beam at GSI:(University of Warsaw)

A semi classical coupled-channel Coulomb excitation least-squares search code GOSIA[7], has been developed to analyze the large sets of experimental data required to unambiguously determine many electromagnetic matrix elements involved in heavy-ion induced Coulomb excitation. The Coulex technique is widely applied to study various nuclei, using both stable beams as well as exotic species accelerated by radioactive beam facilities, and the GOSIA code remains the most reliable and powerful tool for data analysis. To make possible profiting from the advantages of this well-known code during analysis of slowed down beam Coulomb excitation measurements at GSI, a particular data analysis technique and a modification of the GOSIA code are developed in frame of TASK3 of JRA-INTAG.

In the Coulomb Excitation description as well as the γ -decay formalism implemented in GOSIA code it is assumed that the projectile scattering angle and the bombarding energy are constant for a given experiment. The exact reproduction of the experimentally observed γ yields requires integration over a finite scattering angle range and over the range of bombarding energies resulting from the projectile energy loss in a target.

The calculated integrated yields are compared with the ones resulting from a “point” calculation and the obtained correction factors are used to transform the actual experimentally observed yields to the ones to which the subsequent fit of the matrix elements will be made. This operation allows to avoid the time-consuming integration while fitting the matrix elements and is treated as an external level of iteration. The effect of the finite scattering angle and bombarding energy ranges as compared to the “point” values of the yields is not explicitly dependent on the matrix elements, thus the fit can be done to the “point” values and then the integration/correction procedure can be repeated and the fit refined until the convergence is achieved.

Generally it is permitted to integrate over any arbitrary (θ , ϕ) shape of the particle detector, although for more complex set-ups it can be complicated to define the geometry of the detection system.

In particular the PIN option has been implemented to be used when the charged particle detectors comprises an array of small PIN-diodes. This approach has been also successfully applied to describe a very complicated shape of a DSSD system, which was represented as 1143 pixels (see Figure 6) [8].

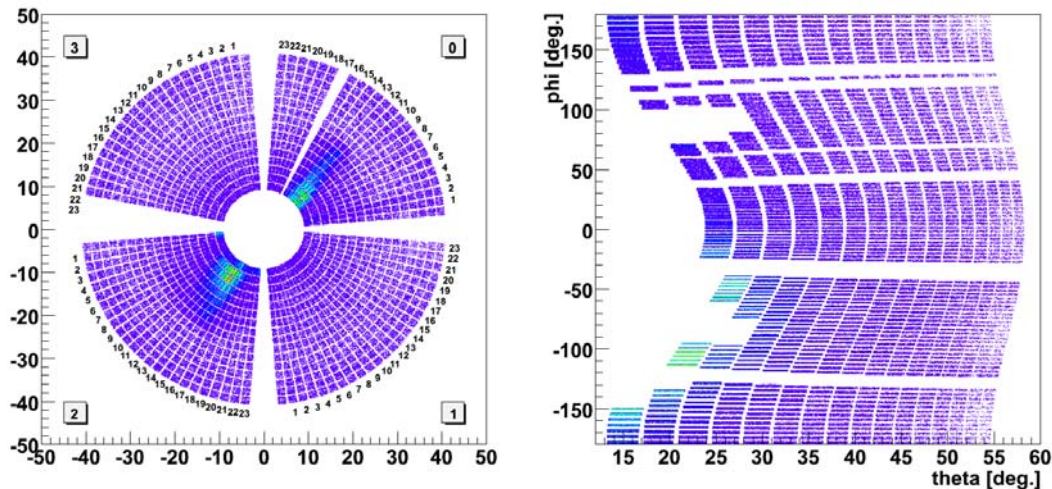


Figure 6. Description of the DSSD detector with PIN option.

A similar technique as shown above is proposed to describe particle detection in slowed down beam experiments. Tracking detectors designed for slowed down beam set-up at GSI provide necessary information for a scattering reconstruction in the event by event mode. Collected particle- γ coincidence data should be sorted into the (θ, ϕ) matrix as it was shown in Figure 6 (right) during offline analysis. The created “virtual detector” can be described using the PIN option, enabling the reproduction of the experimentally observed γ yields.

The (θ, ϕ) distribution of the scattered particles registered in the virtual detector cannot be described by the Rutherford formula. The scattering probability depends on the beam profile on the target and can be measured using downscaled particle events (collected without the particle- γ coincidence condition). The experimental data can be included in GOSIA as a weight parameter in the modified PIN option.

The modification of the GOSIA code is implemented and will be tested with the data from the test experiment performed at the GSI facility in September and October 2008.

Manufacturing and testing of tracking detectors: GSI, Huelva, Seville, Koeln

Based on the simulation results and technical feasibility the following development was performed:

- In-beam test of a diamond detector was performed.
- Two Secondary Electron Detectors with MCP plates were build.
- Fast timing preamplifier developed for diamond detectors were modified to work with 40 micron 5x5 cm² 16x16 strips double sided Si strip detector.

Performance of CVD diamond detectors in beam [9]

Recently, it was shown that SC CVD diamonds permitted of detection of α -particles from a ²⁴¹Am source with good energy resolution, comparable with Si detectors [10]. On the other hand, time of flight measurements of relativistic heavy ions demonstrated that a time accuracy of PC and SC CVD diamond sensors is significantly better than 100 ps.

Here, we report on an in-beam evaluation of a CVD diamond detector sensitivity on low energy and high intensity ion beams: p, and ⁷Li at energies of 5.8 MeV, 8.7 MeV and 11.2 MeV respectively, delivered by the CNA-Seville 3 MV tandem accelerator. SC and PC CVD diamond detectors of a size of 4x4 mm² and 1x1 cm², respectively, and various thicknesses were tested. The projectiles, were Rutherford scattered on thin Al, Pb and Au targets. A SC CVD diamond detector of 500 μ m thickness was positioned at 70 degree with respect to the beam direction. Output signals were shaped in a standard charge sensitive preamplifier. The measured energy spectra of the scattered protons are presented in Fig.7.A. The peak shift and broadening resulted from the target element composition and the energy spread due to the target thickness, as indicated in the picture. However, the spectrum measured for the 1 μ m Al target demonstrates rather narrow distribution of 50 keV at the FWHM,

reaching the energy of 5.55 MeV. These values correspond rather well to the calculated energy spread and the maximum scattered proton energy. Therefore, one may conclude that the intrinsic energy resolution of the SC CVD diamond is better than 50 keV. A stack consisting of a 110 μm and 300 μm SC CVD diamond detectors was mounted at the angle of 90 deg. The protons scattered on the Pb target crossed over the thinner detector, losing half of the kinetic energy and were stopped in the second diamond. Pulses from both detectors were fed into broad band voltage-sensitive preamplifiers DBA2 [11] that provided signals with a few tens ps rise-time. The coincidence rate was 70% of singles, in part due to the detectors misalignment. Leading edge discriminators were used to determine the signal timing. The telescope time correlation spectrum is shown in Fig.8.B. One clearly sees a coincident peak of only 100 ps at the FWHM, even though a walk correction for such fast signals was not feasible. The scattering setup was used to measure a time correlation between a PC CVD diamond detector of 13 μm thickness and the 300 μm SC CVD diamond, mounted in a stack.

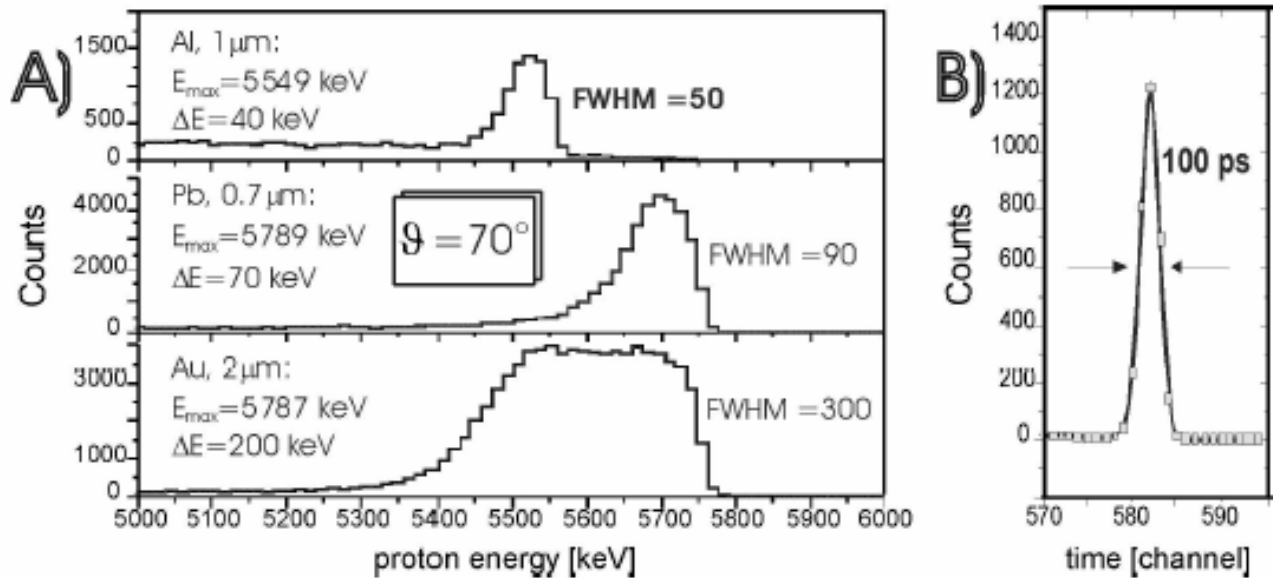


Figure 7 A) Energy spectra of 5.8 MeV protons elastically scattered from different targets, detected by a 500 μm SC CVD diamond detector at 70° . The calculated maximum energy and the peak broadening are indicated. The intrinsic detector energy resolution is below 50 keV, thus better than 1%. B) Time correlation spectrum of two SC CVD diamond detectors irradiated by the scattered proton beam. The time resolution of 100 ps at the full width half maximum and efficiency above 70% were measured.

The ^7Li beam irradiated the Pb target. The projectile range in diamond was 16 μm , the distance comparable with the PC detector thickness. Therefore, one expected high energy deposition of about 10 MeV in this detector. Indeed, despite low charge collection efficiency in a PC diamond, a signal of sufficient amplitude was generated. Although ^7Li ions entered into the second SC CVD diamond with energy below 1 MeV, one could clearly see coincident signals from the two detectors. As in the previous case, the PC and the SC diamonds exhibited very good correlation with the time resolution within the 10^2 ps range. To clarify the diamond detectors ability of detecting ions at high rates the 300 μm SC CVD diamond detector was exposed to direct proton and α -particle beams. The minimum stable current extracted from the accelerator corresponded to a beam flux of the order of 10^7 particles/s $\cdot\text{cm}^2$. Although the irradiation lasted several minutes, DBA2 preamplifier signals monitored on a fast digital oscilloscope exhibited no signs of degradation or noisiness. Negligible leakage current was registered. The detector allowed for a clear distinction of two consecutive signals separated by 10 ns that would correspond to a continuous rate of 100 MHz.

The MCP detectors were tested with alpha source and fission fragment source. In Figure 8(left) a picture of the Secondary Electron Detectors mounted for testing is shown. The detector construction is described in Ref [12] and schematically shown in Figure 8(right).

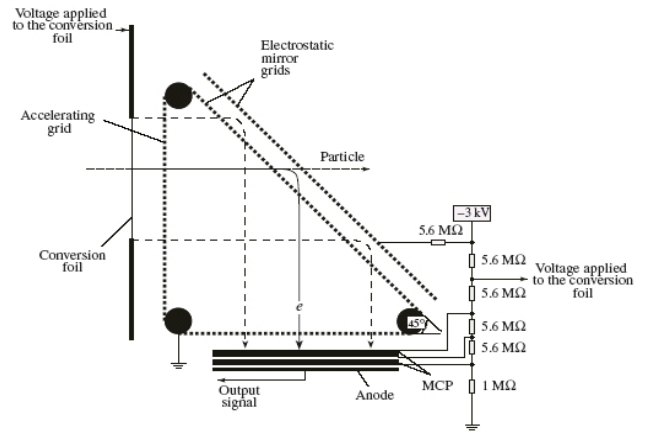
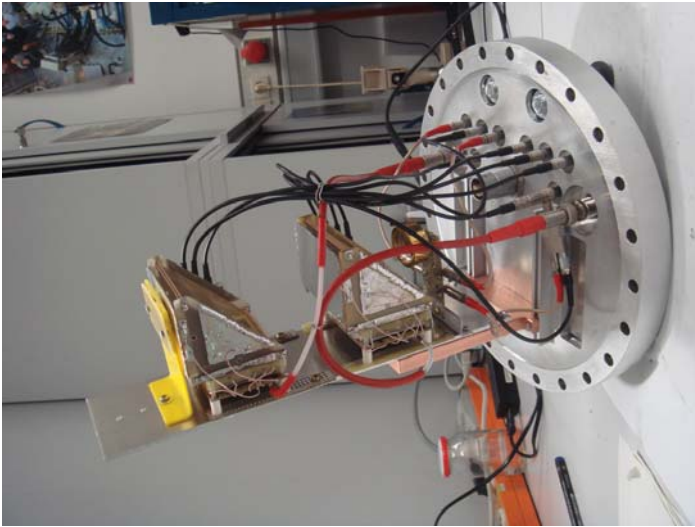


Figure 8: Secondary Electron Detectors built for slow down beam experiments at FRS (left). Schematic drawing of the Secondary Electron Detectors assembly (right).

The measured time resolution with alpha particles was $\Delta T(\text{FWHM}) \sim 140$ ps. The position resolution for alpha particles was $\Delta X_{\alpha}(\text{FWHM}) \sim 3$ mm and $\Delta X_{\text{fr}}(\text{FWHM}) \sim 1.5$ mm for fission fragments.

A prototype fast Si preamplifiers was tested with ^{48}Ca beam at the UNILAC facility at GSI. Coulomb scattering was used to reduce the beam intensity. An estimated timing resolution of $\Delta T(\text{FWHM}) \sim 100$ ps was obtained based on the pulse rise time of 2 ns and the RMS of the nose. A direct ΔT measurement was not possible with the prototypes due to problems with positive feed back at high frequency. The later problem was solved and a full assembly of 16 ch fast preamplifier was build and will be tested.

Commissioning at FRS

Two different setups were used for test at the FRagment Separator at GSI. An experiment in which a 100 μm scintillator was used for TOF detector was performed in Oct 2007. In Figure 9 (right) a photo of the setup is shown. The 100 μm scintillator was positioned at 2.7 m behind the degrader, a second scintillator was placed in front the degrader.

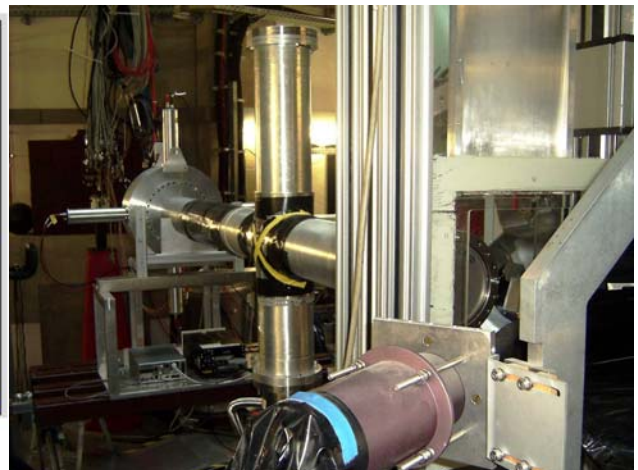
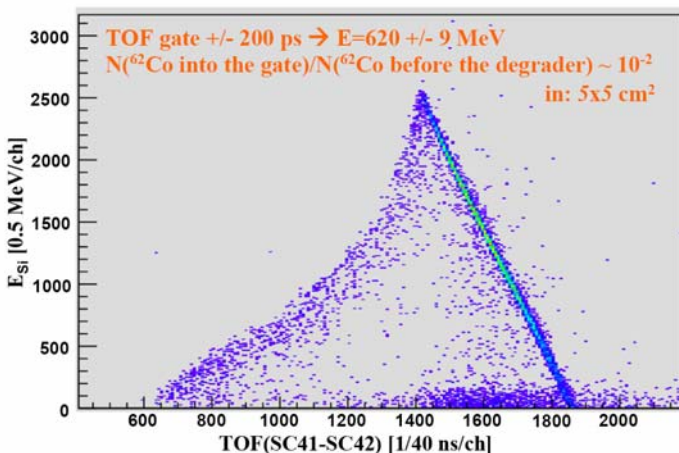


Figure 9: (left) ^{62}Co energy after slowing down versus TOF measurement with 100 micron scintillator detector. (right) Photograph of the test setup with 100 micron scintillator detector used for TOF measurement.

The test shown that time resolution of 141ps can be obtained with the available BC420 scintillator. A 300 μm silicon detector position behind the scintillator was used to determine the energy of the incoming beam. The Si detector was calibrated with the position of the Bragg peak

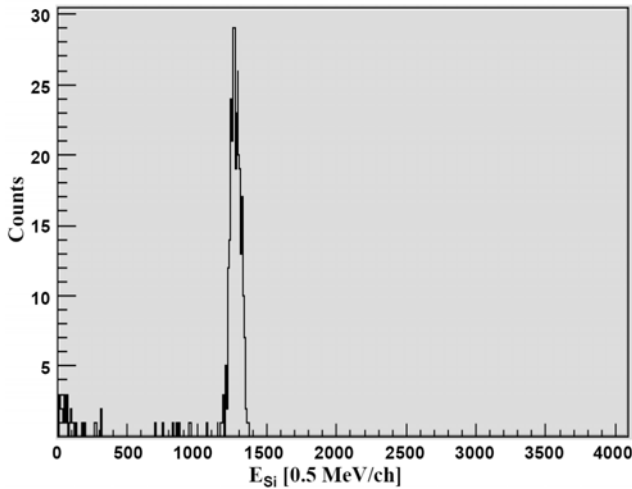


Figure 10: Energy measured in the Si detector after a cut of $\pm 200\text{ps}$ around 10 MeV/u. and the extrapolated point where the beam just starts to give signals in the Si. The width of the energy distribution around 10 MeV/A when applying a cut of $\pm 200\text{ps}$ on TOF was $\sim 80\text{MeV}$ (Figure 10). The theoretically calculated width was 17MeV. This difference was attributed to the variation of the material thickness along the surface of the scintillator.

The width of the beam spot at the TOF detector was 2.0 ± 0.3 time bigger that the beam spot size before the degrader. The theoretically expected increase was 1.7. This indicates that the current Monte-Carlo (MC) simulation may underestimate the angular straggling. The number of counts which were in the TOF gate over the total number of detected ^{62}Co fragments in the Si detector position behind the TOF detector was 6.5%. The expected number from MC simulation was 2.5%. Hence the simulation predicts bigger range straggling compared to the experiment. A possible source for this disagreement is the default material roughness in the MC simulation, which can be optimized in the future.

In September-October 2008 a second test was performed. The detector arrangement for the second setup is shown on Fig 11(right). The detectors were positions at 1.5 m behind the degrader, close to the center of the RISING Ge array.

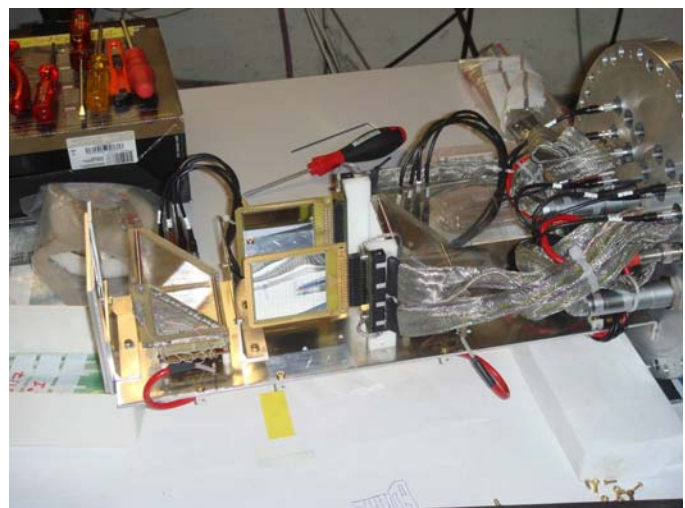
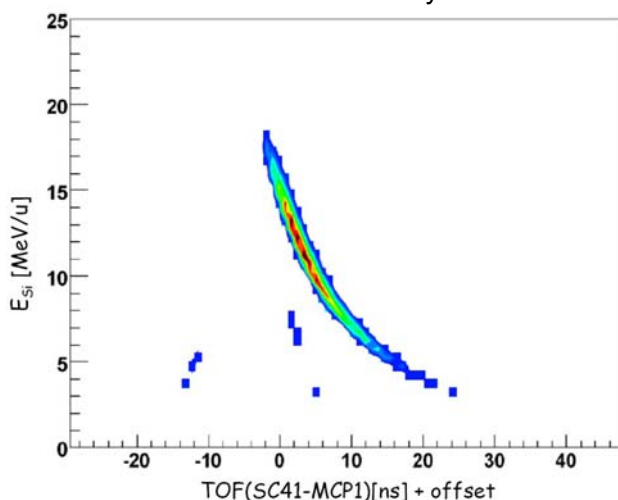


Figure 11 (left) Energy of ^{64}Ni after slowing down deterged from a TOF measurement with Secondary Electron Detector. (right) Detector arrangement used for Coulomb excitation measurement. A collimator on the left is followed by an MCP detector, a gold target, two DSSSD detectors parallel to the beam and a second MCP detector. NaI detectors were placed around the gold target.

The experiment utilized the MCP detectors described in the previous section, 2 DSSSD detectors and NaI detectors. The averaged beam intensity on target was about 10^5 pps. The rate was limited by the response of the scintillator used for start of the TOF measurement, positioned in front of the degrader. The test provided information on the performance at high rates of the auxiliary FRS detectors (TPC, MUSIC and scintillator detectors) used for beam tracking before the degrader.

In Figure 11 the energy spectrum after slowing down is shown determined with a $300\ \mu\text{m}$ Si detector versus the TOF between the scintillator in front of the degrader and a the first MCP detector upstream from the target position. The energy spread in Figure 11 is smaller compared to the analogous measurement shown in Figure 9(left). In the latter the energy distribution is broader due to the straggling in the $100\ \mu\text{m}$ scintillator.

The data is presently under analysis and will provide an answer of the feasibility of Coulomb excitation experiments with the proposed approach.

Momentum selection of spin-aligned isomeric beams in the FRS spectrometer (KU Leuven, University of Sofia, CSNSM, IN2P3/CNRS, GSI)

During the g-RISING experimental campaign for g-factor studies of isomeric states in the Sn and Pb region, the momentum selection has been performed with a position sensitive scintillator at the dispersive focal plane of FRS.

The magnetic moment ($\mu=g.l$) is a very sensitive probe of the nuclear single particle configuration of the nuclear state (with spin l) because the nucleon g-factor depends strongly on their orbital and total momentum. In earlier projectile fragmentation reactions at intermediate and relativistic beam energies, positive spin-alignment has been observed for isomers selected in the centre of their longitudinal momentum distribution and negative alignment in the wing of the distribution. It has been done by selecting the fragment momentum distribution using slits at the dispersive focal plane of the spectrometer.

In the relativistic fission of a ^{238}U beam, spin-alignment has never been demonstrated. However, it is well-known that in spontaneous fission a strong correlation exists between the emission direction of the γ -ray and that of the fission fragment. It can therefore be expected to observe also spin-alignment in a selected ensemble of relativistic fission fragments. In the present studies the momentum selection was achieved using the position sensitivity of a scintillation detector (Sci S2) placed at the same position in the spectrometer. The scintillator at S2 consists of a plastic piece (BC420) with a size of $220 \times 45\ \text{mm}^2$. The thickness used in the experiments is of 3.37 mm. Two photo multipliers (H2431/R2083) are used horizontally on the left and the right sides in order to read out the scintillation light. During these runs the particle rate at S2 was kept almost constant of about 2×10^5 p/s distributed in 8s spill length with a period of 20 s, while the dose from the beginning until the end of the run is increased from about 2×10^8 p to about 5×10^{10} p. A consecutive study during to whole experiment showed that there were no abrupt changes in the particle rate and therefore the deterioration in energy response of the S2 scintillator was an effect of the collected dose. Observed was not only signal deterioration but also shift of the energy signal, which could be a consequence of e.g. the drop of the effective HV due to fluctuations in the particle rate.

The X position of the ^{127}Sn ions at the S2 scintillator in the beginning and the end of the fragmentation run are shown in Fig. 12(a) and Fig. 12(b), respectively. Due to the deteriorated shape in order to select the centre or the wing of the momentum much narrower cuts have to be made, which reduce the statistics for g-factor analysis. The effect of the momentum selection is demonstrated in Fig. 12(c) for cut in the centre and in Fig. 12(d) for cut in the wing of the distribution for one of the strongest (the ground state 1095 keV E2 transition in ^{127}Sn which follows the decay of the $4.5\ \mu\text{s}$ $19/2^+$ isomer [13]). As it can be seen, the amplitude of the $R(t)$ oscillation function, from which the g-factor of the decaying isomeric state can be obtained, is much smaller in the centre than in the wing of the momentum distribution. It is interesting to note also that the isomeric ratio (amount of isomeric γ -rays) is also increased in the wing of the distribution with about 25% as is shown with the blue curves in Fig. 12(a,b).

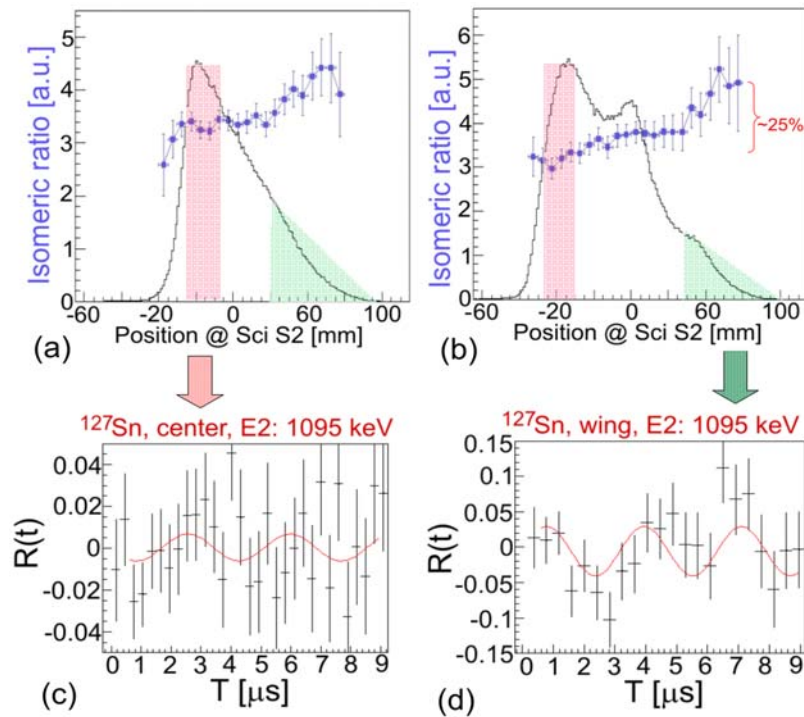


Figure 12. Momentum distribution (a) at the beginning and (b) the end of the fragmentation run. The $R(t)$ functions for the ground state $E2$ transition in ^{127}Sn is shown for a momentum selection (c) in the centre and (d) the wing.

The response of the S2 scintillator during the g-RISING studies showed that currently 10^4 p/s seems to be the maximum rate which can be handled at S2 without a loss of performance. Rates of 10^5 - 10^6 p/s at S2, which were used in these studies, showed instability of the detector's gain. The collected particle dose seems to be limited to 10^{10} p, after which a recovery time is needed.

References

- [1] S. Tashenov, J. Gerl, Nucl. Instrum. Methods Phys. Res. A 586, 224 (2008).
- [2] P. Medina et al., "TNT Digital Pulse Processor", 14th IEEE-NPSS Real Time Conference 20054, Stockholm, Sweden, 6-10 juin 2005
- [3] L. Arnold et al., IEEE Trans. Nucl. Sci., **53**, 723 (2006)
- [4] M. Górska et al., Acta Phys. Pol. B38, 1219 (2007).
- [5] P. H. Regan et al., Nucl.Phys. A787, 491c (2007).
- [6] H. Geissel, et al., Nucl. Instr. and Methods Phys. Res. B 70, 286 (1992).
- [7] T. Czosnyka, D. Cline, C.Y. Wu - Bull. Am. Phys. Soc. 28:745 (1983)
- [8] M. Zielińska et al., *Determination of nuclear static moments using post-accelerated exotic beams: Coulomb excitation of neutron-rich ^{44}Ar at SPIRAL*, EURONS Town meeting, Rhodes, Greece, 2008; M. Zielińska et al., *Complicated particle detector geometry and normalization to target excitation*, GOSIA Workshop, Warszawa, Poland, 2008.
- [9] P. Bednarczyk et al., Acta Phys. Pol. B38, 1293 (2007).
- [10] M. Pomorski et al., Phys. Stat. Sol. A 202, 2199 (2006)
- [11] P. Moritz et al., Diamond Relat. Mater. 10, 1765 (2001);
- [12] E.M Kozulin et al, Instr. And Expt. Techniques Vol. **51**, No. 1
- [13] J. Pinston et al, Phys. Rev. C **61**, 024312 (2000)

Conference presentations

"Application of Diamond Detectors in Tracking of Heavy Ion Slowed Down Radioactive Beams"

B. Bednarczyk, Talk at **Zakopane Conference on Nuclear Physics**

Trends in Nuclear Physics, 4-10 September, 2006, Zakopane, Poland

<http://www.zakopane2006.ifj.edu.pl/>

"Simulations and test results of the slowed down beams projects at GSI"

P. Boutachkov, Talk at the **DPG**

DPG conference

10-14 March, 2008, Darmstadt – Germany

http://www.dpg-verhandlungen.de/2008/darmstadt/index_en.html

"Development of slowed down beams at GSI"

P. Boutachkov, Talk at **EURORIB'08**

8-13 June, 2008, Giens-France

<http://eurorib08.ganil.fr>

Milestone Table

Milestones	Milestone names	Date due	Date accompl
M-J06.3.1	Design of tracking detectors	18	18
M-J06.3.2	Manufacture of tracking detectors	30	30
M-J06.3.3	Tests of tracking detectors	33	33
M-J06.3.4	Commissioning at FRS and Coulex analysis	42	46
M-J06.3.5	Design of segmented planar Ge	18	18
M-J06.3.6	Manufacture of segmented planar Ge	30	
M-J06.3.7	Tests of segmented planar Ge	33	
M-J06.3.8	Commissioning at FRS	42	46
M-J06.3.8	Simulation for design studies	18	18